optica

Role of epsilon-near-zero substrates in the optical response of plasmonic antennas: supplementary material

Jongbum Kim[1], Aveek Dutta[1], Gururaj V.Naik[1], Alexander J. Giles[2], Francisco J. Bezares[2], Chase T. Ellis[2], Joseph G. Tischler[3], Ahmed M. Mahmoud[4], Humeyra Caglayan[5], Orest J. Glembocki[3], Alexander V. Kildishev[1], Joshua D. Caldwell[3], Alexandra Boltasseva[1] and Nader Engheta[4]

[1]School of Electrical and Computer Engineering and Birck Nanotechnology Center, Purdue University, West Lafayette, IN 47907, USA

[2]NRC/ASEE – NRL Postdoctoral Fellows, Naval Research Laboratory, Washington, D.C. 20375, USA

[3]Electronic Science & Technology Division, Naval Research Laboratory, Washington, D.C. 20375, USA

[4]Department of Electrical and Systems Engineering, University of Pennsylvania, Philadelphia, Pennsylvania 19104, USA

[5]Electrical and Electronics Engineering, Abdullah Gul University, Kayseri, 38080, Turkey

*Corresponding author: engheta@ee.upenn.edu

This document provides supplementary information to "Role of epsilon-near-zero substrate in the optical response of plasmonic antennas," http://dx.doi.org/optica.3.000339. A detailed discussion of sample preparation and optical characterization for TCOs and SiC experiments, methods for numerical modeling and analytical methods for calculation of effective permittivity are presented, along with additional experimental data on cross-polarized reflection of nanorod antenna array on TCOs substrates. © 2016 Optical Society of America

Transcparent Conducting Oxides (TCOs)

Sample preparation: Undoped ZnO, Ga:ZnO and Al:ZnO films were deposited by pulsed laser deposition (PVD Products, Inc.) using a KrF excimer laser (Lambda Physik GmbH) operating at a wavelength of 248 nm for source material ablation. The energy density of the laser beam at the target surface was maintained at 1.5 J/cm^2 and an oxygen partial pressure is 0.05 mTorr. The substrate temperature during TCO thin film deposition was maintained at 70 ^{0}C. To fabricate Au nanorod antenna, positive electron beam resist (ZEP 520 A) was spin-coated at 4000 r/min and then exposed by electron beam lithography (Vistec VB6). The beam energy was 100 kV and the beam current was 1.012 nA. The base dose was maintained at 320 μC/cm^2. 40-nm-thick Au film was deposited on the resist with electron beam evaporator. The sample was developed in ZED-N50 (n-amyl acetate) for 1 min, and dipped in isopropyl alcohol for 30 s to rinse ZED-N50, and then dried in gaseous nitrogen.

Optical characterization: The optical properties of the TCOs and ZnO films were characterized by spectroscopic ellipsometry (V-VASE, J. A. Woollam) in the spectral region from 350 to 2500 nm. The dielectric function of the films were retrieved by fitting a Drude + Lorentz oscillator model to the ellipsometry data and the optical constants for Au were obtained from Rakic [1]. The following equation describes the Drude + Lorentz oscillator model where the second term comes from the Drude model and the third term represents the Lorentz oscillator. The retrieved model parameters are listed in Table S-1.

$$\varepsilon(\omega) = \varepsilon_\infty - \frac{\omega_p^2}{\omega(\omega + i\Gamma_p)} + \frac{f_l\omega_l^2}{\omega_l^2 - \omega^2 - i\omega\Gamma_l}$$

Table. S-1. Drude + Lorentz model parameters for TCOs

	ε_∞	ω_p (eV)	Γ_p (eV)	f_l	ω_l (eV)	Γ_l (eV)
AZO	2.231	1.512	0.084	1.057	5.127	0.062
GZO	2.321	1.989	0.090	0.960	5.021	0.001

The cross-polarized reflection according to incident light was also measured with the ellipsometry at 20^0 angle of incidence. While rotating the detector from 20^0 to 340^0, the radiation pattern was characterized by collecting the intensity of cross-polarized reflection for upside substrate and transmission for downside substrate.

Silicon Carbide (SiC)

Antenna Array Fabrication: Au nanoantennas were patterned on both a semi-insulating 4H-SiC substrate from Cree Inc. and on an p-type Si substrate using electron beam lithography. The 40-nm-thick gold antennas were fabricated using electron beam deposition, with a 3 nm thick titanium layer used to improve adhesion. In all cases the arrays were periodic and the antennas had a constant aspect ratio of 4. The periodicity was equivalent in the x and y directions for a given array and was defined as 1000 nm longer than the antenna length.

Optical Characterization: Using a 50 μm x 50 μm aperture within both a Thermoscientific Nicolet Continuum and a Bruker Infineon FTIR microscope, the reflectance spectra from each of the arrays was collected both in reference to Au and to the surrounding SiC substrate. In the case of the cross-polarized spectra, the incident (excitation) light was linearly polarized at 45° with reference to the antenna principle axes and collected through a polarizion analyzer rotated 90°. This orientation was required to ensure that both the excitation and analyzer were sensitive to radiation polarized along the long-axis of the nanorod. Control measurements were performed with only the excitation polarization along both the short and long axis of the nanorod and verified that the resonance was only observed with the latter. These measurements also verified that the increase in the LO phonon amplitude and the Fano-interference were only observed with linear polarization along the long-axis.

Electromagnetic Modeling

In order to understand the influence of the ENZ effect upon the antenna resonance and radiation pattern, 3D electromagnetic simulations of the reflectivity and near-field distributions of electromagnetic fields of the structure were performed using the finite-element method (FEM) with commercial software (COMSOL Multiphysics®) for TCO modeling and the finite-difference time-domain (FDTD) for SiC. The FDTD simulations were performed using Lumerical Solutions® software. The optical constants for Au were obtained from Etchegoin et al. [2] and Rakic [1]. The dielectric functions of SiC were calculated by the model from Tiwald et al [3], while those for the TCOs were derived using ellipsometry. Because the arrays were periodic, the simulations used periodic boundary conditions and the light was polarized along the long-axis of the antenna.

Calculations of the Effective Index and Effective Antenna Length

The effective antenna length and index of the ENZ and dielectric substrates were calculated using Eq (1) in the main text. For the purposes of calculating the effective index, two approximations may be used. The first, proposed by Novotny [4], approximates the effective permittivity as $n_{eff} = \sqrt{(\varepsilon_{sub} + \varepsilon_{air})/2}$, while the second, proposed by Neubrech et al. [5], is represented as $n_{eff} = \sqrt{(\sqrt{\text{Re}(\varepsilon_{eff})^2 + \text{Im}(\varepsilon_{eff})^2} + \text{Re}(\varepsilon_{eff}))/2}$. While both approximations offer equally accurate results when $\text{Re}(\varepsilon) > 1$,

the latter approximation is required to achieve reasonable agreement with experiment when $\text{Re}(\varepsilon) \rightarrow 0$. This is due to the increasing importance of the magnitude of the imaginary part of the dielectric function in determining n_{eff} under these conditions.
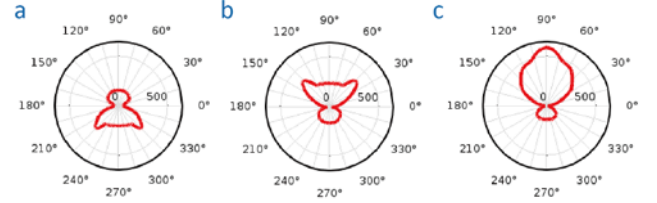
Radiation pattern of 2D antenna

Fig. S-1. Radiation pattern of a 2D antenna on substrates with different $Re(\varepsilon)$**.** *The radiation pattern of a two dimensional antenna (infinitely long wire) placed on the interface between air and a semi-infinite (loss-less) dielectric medium with relative dielectric constant of (a)* $Re(\varepsilon) = 2$*, (b)* $Re(\varepsilon) = 0.5$*, (c)* $Re(\varepsilon) = 0$

The radiation patterns of 2D antennas on substrates with a different real part of permittivity are simulated as shown in Fig. S-1. The radiation in the presence of the dielectric substrate (Fig. S-1a) is emitted over a large solid angle, with primary beams directed at 45° and -45° off normal, being scattered into primarily the substrate. However, when the antenna is placed on the substrate of which permittivity is less than 1 but greater than zero, the radiation behavior is effectively inverted. As the permittivity approaches zero, the radiation from the antennas is mostly back-scattered into the ambient (air) as shown in Fig. S-1c.

The impact of imaginary part of permittivity (optical losses) on the electric field magnitude patterns of antenna.
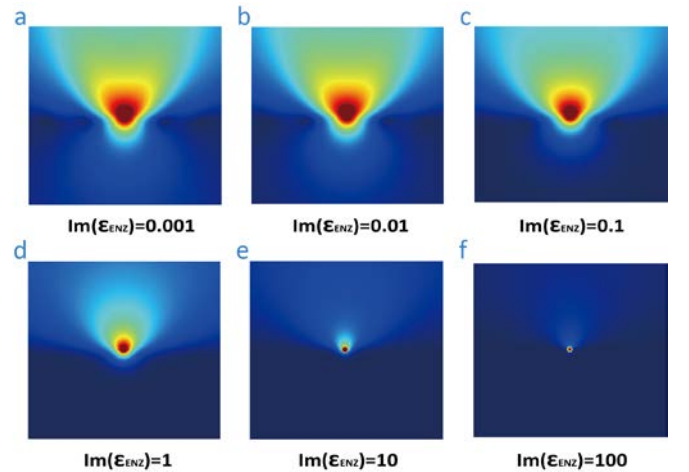

Fig. S-2. Electrical field magnitude of a 2D antenna on substrates with different $\text{Im}(\varepsilon)$ **at the ENZ wavelength.** The electrical field magnitude pattern of a two dimensional antenna (infinitely long wire) placed at the interface between air and a epsilon near zero ($\text{Re}(\varepsilon) = 10^{-4} \approx 0$) medium with relative imaginary part of permittivity of (a) $\text{Im}(\varepsilon) = 0.001$, (b) $\text{Im}(\varepsilon) = 0.01$, (c) $\text{Im}(\varepsilon) = 0.1$, (d) $\text{Im}(\varepsilon) = 1$, (e) $\text{Im}(\varepsilon) = 10$ and (c) $\text{Im}(\varepsilon) = 100$.

The influence of imaginary part of permittivity ($\text{Im}(\varepsilon)$) of an ENZ substrate upon the electric field magnitude pattern of a local antenna is of interest because this study is highlighted on the practical ENZ materials with low optical losses. Figure S-2 depicts the simulation results of the electrical field magnitude pattern of 2D antenna sitting on the ENZ substrate with

different value of Im (ε). As the imaginary part of the permittivity of the substrate increases, the substrate behaves more and more like an electric conductor, and thus the field generated by the antenna would diminish, similar to the case of making the real part of permittivity more and more negative, as shown in Fig. 1.

Cross-polarized reflection from nanorod antenna with fixed gap between neighboring antennas.
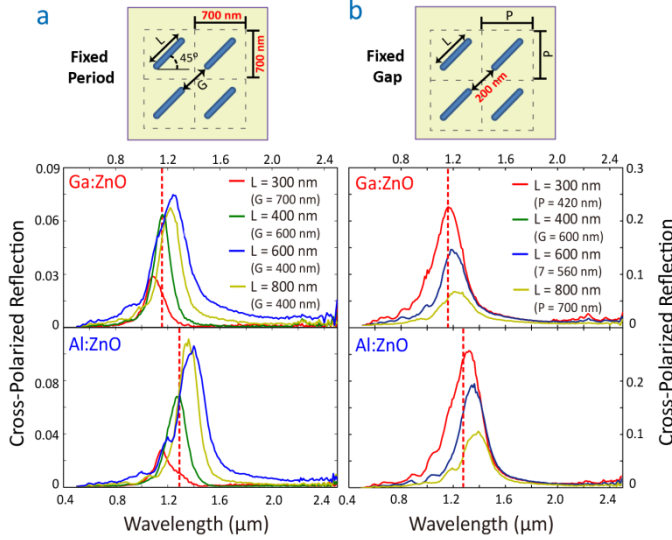

Fig. S-3. Comparison of optical characterization of nanorod antenna arrays on TCOs with different designs. Experimental cross-polarized reflection spectra of Au nanorod arrays, fabricated on TCOs (Ga:ZnO and Al:ZnO) with (a) fixed period (P = 700 nm) and (b) fixed gap (G = 200 nm). Vertical Red dashed line indicates the ENZ points for Al:ZnO and Ga:ZnO.

To observe the effect of resonance behavior with respect to antenna design, we fabricated nanorod arrays with two different cases; fixed gap between the end of nanorods and fixed period. In both cases, the length of nanorods differs from 300 to 800 nm. The corresponding cross-polarized resonance spectra are provided in the Fig. S-3. In the both cases, we can clearly observe the 'pinning' of resonance wavelength at the ENZ wavelength. The difference between two cases is the peak intensity of reflection. For the case of the fixed period, the number of antennas per unit area is the same, thus the slight variation in the peak intensity is due to different lengths of the antennas. However, for the case of the fixed gap, the period p changes with the antenna length, being 700 nm, 560 nm and 420 nm for antenna lengths of 800 nm, 600 nm and 400 nm respectively. Therefore the number of antennas per unit area is drastically increasing as we change antenna length from 800 nm to 400 nm, and it leads to a larger variation in the measured peak intensity.

Comparison of co-polarized reflection and cross-polarized reflection from nanorod antenna on Al:ZnO substrate

Figure S-4 depicts the reflection spectra of the overlying Au antennas on Al:ZnO substrate. Analogous to the results from the 4H-SiC as shown in Fig. 6, we observe the increase of the co-polarized reflection from the nanorod antenna at the slope of reflection spectra near ENZ wavelength. However, it is difficult to identify the reflection of antenna from the co-polarization measurement due to the strong reflection from Al:ZnO substrate. In contrast to co-polarized reflection measurement, both the co-polarized and cross-polarized reflection provides a well-defined

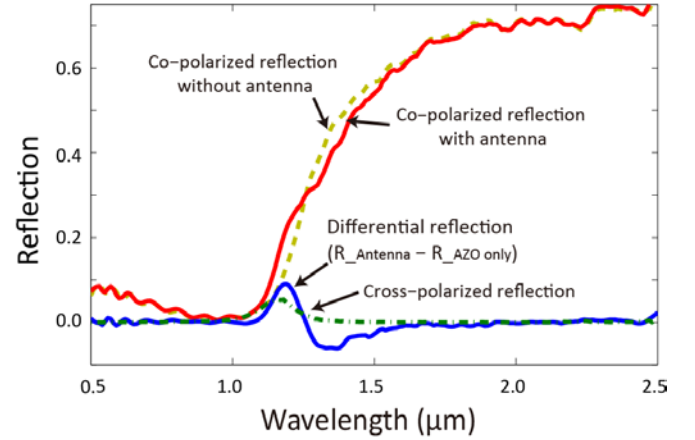*resonance peak from the antenna by cancelling out the signal from the substrate.*

Fig. S-4. Reflection spectra from nanorod antenna with 400 nm lenth. *(red solid line) co-polarized reflection with antenna array on Al:ZnO substrate (yellow dashed line) co-polarized reflection from Al:ZnO substrate without antenna array. (blue solid line) co-polarized differential reflection ($R_{Antenna} - R_{AZO\,only}$) (green dashed line) Cross-polarized reflection from antenna on Al:ZnO substrate.*

REFERENCES

1. A.D. Rakic, "Algorithm for the determination of intrinsic optical constants of metal films: application to aluminum," *Appl. Opt.* **34**, 4755-4767 (1995).
2. P.G. Etchegoin, E. Le Ru, and M. Meyer, "An analytic model for the optical properties of gold," *J. Chem. Phys.* **125**, 164705 (2006).
3. T. E. Tiwald, J. A. Woollam, S. Zollner, J. Christiansen, R. B. Gregory, T. Wetteroth, S. R. Wilson, and Adrian R. Powell. "Carrier concentration and lattice absorption in bulk and epitaxial silicon carbide determined using infrared ellipsometry," *Phys. Rev. B* **60**, no. 16, 11464 (1999).
4. L. Novotny, "Effective wavelength scaling for optical antennas," *Phys. Rev. Lett.* **98**, 266802 (2007).
5. F. Neubrech, T. Kolb, R. Lovrincic, G. Fahsold, A. Pucci, J. Aizpurua, T. Cornelius, M. Toimil-Molares, R. Neumann and S. Karim, "Resonances of individual metal nanowires in the infrared," *Appl. Phys. Lett.* **89**, 253104 (2006).